Cardiovasc Toxicol (2010) 10:27–36
DOI 10.1007/s12012-009-9060-4

Nanoparticle Inhalation Impairs Coronary Microvascular Reactivity via a Local Reactive Oxygen Species-Dependent Mechanism

A. J. LeBlanc · A. M. Moseley · B. T. Chen · D. Frazer · V. Castranova · T. R. Nurkiewicz

Published online: 22 December 2009

Abstract We have shown that nanoparticle inhalation impairs endothelium-dependent vasodilation in coronary arterioles. It is unknown whether local reactive oxygen species (ROS) contribute to this effect. Rats were exposed to TiO_2 nanoparticles via inhalation to produce a pulmonary deposition of 10 μg. Coronary arterioles were isolated from the left anterior descending artery distribution, and responses to acetylcholine, arachidonic acid, and U46619 were assessed. Contributions of nitric oxide synthase and prostaglandin were assessed via competitive inhibition with N^G-Monomethyl-L-Arginine (L-NMMA) and indomethacin. Microvascular wall ROS were quantified via dihydroethidium (DHE) fluorescence. Coronary arterioles from rats exposed to nano-TiO_2 exhibited an attenuated vasodilator response to ACh, and this coincided with a 45% increase in DHE fluorescence. Coincubation with 2,2,6,6-tetramethylpiperidine-N-oxyl and catalase ameliorated impairments in ACh-induced vasodilation from nanoparticle exposed rats. Incubation with either L-NMMA or indomethacin significantly attenuated ACh-induced vasodilation in sham-control rats, but had no effect in rats exposed to nano-TiO_2. Arachidonic acid induced vasoconstriction in coronary arterioles from rats exposed to nano-TiO_2, but dilated arterioles from sham-control rats. These results suggest that nanoparticle exposure significantly impairs endothelium-dependent vasoreactivity in coronary arterioles, and this may be due in large part to increases in microvascular ROS. Furthermore, altered prostanoid formation may also contribute to this dysfunction. Such disturbances in coronary microvascular function may contribute to the cardiac events associated with exposure to particles in this size range.

KeyWords Microcirculation · Nanoparticle · Coronary · Arteriole · Vasodilation · Titanium dioxide · Inhalation · Reactive oxygen species

A. J. LeBlanc · T. R. Nurkiewicz (✉)
Center for Cardiovascular and Respiratory Sciences, 1 Medical Center Drive, Robert C. Byrd Health Sciences Center, West Virginia University School of Medicine, Morgantown, WV 26506-9105, USA
e-mail: tnurkiewicz@hsc.wvu.edu

A. J. LeBlanc · D. Frazer · T. R. Nurkiewicz
Department of Physiology and Pharmacology, West Virginia University School of Medicine, Morgantown, WV 26506, USA

T. R. Nurkiewicz
Department of Neurobiology and Anatomy, West Virginia University School of Medicine, Morgantown, WV 26506, USA

A. M. Moseley · B. T. Chen · D. Frazer · V. Castranova
Pathology and Physiology Research Branch, Health Effects Laboratory Division, National Institute for Occupational Safety and Health, Morgantown, WV 26505, USA

Introduction

Pulmonary exposures to nanoparticle aerosols are currently most notable in occupational and industrial settings. However, given the rate at which nanotechnology is permeating modern society, it is reasonable to expect that the likelihood of these exposures occurring in personal, domestic, and environmental settings will increase in the near future. Therefore, it is critical to identify such health effects now, prior to the establishment of widespread, public exposures as has happened for example with asbestos [1].

We have previously shown that nanoparticle inhalation impairs endothelium-dependent vasodilation in coronary arterioles [2]. The titanium dioxide particles used in our

experiments (Degussa P25, Aeroxide) are commercial nanoparticles, and because dose-dependent pulmonary effects have been well studied, they have also served as a surrogate for the ultrafine particle component of aerosols. Therefore, it is important to characterize the systemic effects of such exposures in relation to the context of the known morbidity and mortality associations with particles of this size range [3]. Changes in the vasoreactivity of coronary arterioles after pulmonary nanoparticle exposure could potentially exacerbate acute coronary event risks. Unfortunately, a limited amount of research investigating how exposure to nanoparticles affects the coronary microvascular network has been performed. One potential route may be through perturbations in reactive oxygen species (ROS), which have previously been shown to be associated with myocardial ischemia [4, 5] and infarct [6]. Additionally, exposure to nanoparticles is thought to be inherently more physiologically dire than their larger counterparts due to their increased surface area and higher pulmonary deposition [7–9]. Consistent with this, we have also shown that pulmonary nanoparticle exposure produces significantly greater systemic microvascular dysfunction than pulmonary exposure to fine particles [8]. What remains to be determined is whether these observations are consistent with microvascular reactivity in critical organs such as the heart.

Altered vasoreactivity in coronary arterioles could alter cardiac activity from several perspectives, but the underlying theme is metabolism. Myocardial anaerobic tolerance is very limited, and normal myocardial function is dependent on a constant supply of oxygen from the coronary circulation [10]. Local metabolic feedback, specifically the production of relaxing and constricting factors, is the primary regulator of coronary blood flow. Due to the high oxygen extraction at rest (~75%), increases in cardiac metabolism must be met by an immediate increase in coronary blood flow or myocardial ischemia can occur. Because we have previously shown that nanoparticle inhalation alters the vasoreactivity of coronary arterioles [2], spatial distribution and volumetric blood supply to the subendocardium may be compromised during periods of increased metabolic demand. Vascular endothelial dysfunction has previously been shown to contribute to the myocardial dysfunction that occurs in pathological states, such as ischemia–reperfusion [11]. Specifically, an absent or inadequate vasodilator response can result in the loss of myocardial contractile efficacy [11]. Accordingly, particle exposure can compound preexisting pathological states. Cozzi et al. (2006) [12] found that exposure to ultrafine (UF) particles doubled the size of myocardial infarction compared to mice treated with vehicle. While ischemic events are ultimately functions of the microcirculation, the mechanisms through which particle exposure induces changes in coronary microvascular reactivity have not been elucidated. This is largely because these mechanisms have not been properly identified in appropriate experimental models.

Myocardial ischemia can arise from a variety of causes, but endothelial dysfunction and heightened smooth muscle cell reactivity are among the most prominent vascular origins of ischemic events [13]. Bartoli et al. [14] recently reported that particle inhalation exacerbates myocardial ischemia. This effect was associated with increased coronary vascular resistance and therefore decreased the myocardial perfusion, but the mechanisms responsible for this effect are not well identified. Therefore, the primary focus of the current study is to identify cellular mechanisms that impair endothelium-dependent vasodilation after nanoparticle exposure. Reactive oxygen species, including hydrogen peroxide (H_2O_2) and superoxide (O_2^-) are produced by a variety of cellular oxidative processes such as NAD(P)H oxidases and the metabolism of arachidonic acid by cyclooxygenases and lipoxygenases [15]. Excess oxidative stress results when the formation of ROS exceeds the capacity of endogenous buffering components. Mice that overexpress antioxidants such as superoxide dismutase (SOD, which converts O_2^- into H_2O_2) incur smaller infarct size than their wild-type counterparts [16]. Endogenous ROS formation can also occur through the arachidonic acid pathway and subsequent cytochrome p-450 activity. Cytochrome p-450-dependent mechanisms generate ROS and therefore similarly influence vascular vasoreactivity [17–19]. The most notable reaction in this regard is O_2^--dependent formation of H_2O_2, a potent vasoactive compound in the coronary vasculature [20].

Numerous origins of ROS production exist, and it has proven difficult to identify a singular point of origin in regard to a specific biologic response. Given this inherent complexity, we have focused on local mediators of reactive species and shown in the skeletal muscle microcirculation that nanoparticle inhalation stimulates local ROS generation via myeloperoxidase and NAD(P)H oxidase activity [21]. Because local ROS generation (independent of its source) can influence vascular reactivity, we hypothesized that excessive coronary ROS production after nanoparticle inhalation could impair endothelium-dependent arteriolar reactivity. Such a microvascular consequence would be consistent with ischemic events that render the greater organ unable to effectively meet demands for alterations in cardiac output.

Therefore, the purpose of this study was to quantify the local oxidative stress in the coronary microvasculature after pulmonary nanoparticle exposure and determine the degree to which these local ROS changes influence arteriolar reactivity in this critical microvascular bed. Because the arachidonic acid pathway is equally important in this

regard, we also characterized alterations in arteriolar reactivity associated with this pathway.

Materials and Methods

Experimental Animals

Specific pathogen-free male Sprague–Dawley [Hla:(SD) CVF] rats (10–12 weeks old) were purchased from Hilltop Laboratories (Scottdale, PA) and housed in an AAALAC approved animal facility at the National Institute for Occupational Safety and Health. Rats were housed in laminar flow cages under controlled temperature and humidity conditions and a 12-h light/12-h dark cycle. Food and water were provided ad libitum. Rats were acclimated for 5 days before use and certified free of endogenous viral pathogens, parasites, mycoplasms, *Helicobacter*, and CAR bacillus. To ensure that all methods were performed humanely and with regard to alleviation of suffering, all experimental procedures were approved by the Animal Care and Use Committees of the National Institute for Occupational Safety and Health, and West Virginia University.

Inhalation Exposure

The inhalation exposure system used for particle exposures in the current experiments has been previously described [8]. Briefly, the system contains a fluidized-bed powder generator (TSI Inc, Shareview, MN), a whole-body animal exposure chamber, and assorted aerosol monitoring and control devices that are collectively capable of generating and characterizing nanoparticle aerosols. Nano-TiO_2 powders were obtained from DeGussa (Aeroxide TiO_2, P25, Parsippany, NJ). This powder is 80% anatase and 20% rutile, with a primary particle size of 21 nm. These proportions of anatase and rutile TiO_2 have been independently verified [22, 23]. Prior to aerosol generation, the dry, nano-TiO_2 particles had BET surface areas [24] of 48.08 m^2/g [25]. The count mode diameter (CMD) of the aerosolized nano-TiO_2 was 100 nm [8]. Up to 3 rats were simultaneously housed in individual compartments of the exposure chamber (food and bedding were absent) for 240 min at aerosol concentrations of 6 mg/m^3. These conditions produced actual lung burdens of 10 μg which were previously measured in ashed lung tissue [8]. The aerosol/exposure profile and particle depositions/burdens for a complete nano-TiO_2 dose–response can be found in the study by Nurkiewicz et al. For the purpose of consistency among ongoing studies, the lung burden of 10 μg produces approximately a 50% impairment in endothelium-dependent vasodilation (EC_{50}) and has been used throughout ongoing experimental series [8, 21].

Subepicardial Arteriole Isolation

After 24-h exposure, rats were anesthetized (thiopental, 100 mg/kg, i.p.), and the heart was removed from the chest. The heart was flushed of excess blood, placed in a dissecting dish with physiological salt solution [PSS (in mmol/l): 129.8 NaCl, 5.4 KCl, 0.5 NaH_2PO_4, 0.83 $MgSO_4$, 19 $NaHCO_3$, 1.8 $CaCl_2$, and 5.5 glucose], and chilled to 4°C. Coronary resistance arterioles from the left anterior descending (LAD) artery distribution were isolated and cannulated as described previously [2]. Arterioles were pressurized to 45 mm Hg [26] with PSS using a servo controlled peristaltic pump (Living Systems Instrumentation, Burlington, VT) and superfused with oxygenated 37°C PSS at a rate of 10 ml/min. Vessel diameter was measured with a video caliper (Colorado Video, Boulder, CO). Vessels without leaks were allowed to develop spontaneous tone (≥20% less initial diameter).

The orders of the following experimental periods were randomized in each vessel to ensure that responses were neither interactive nor time-dependent. Once a vessel had been exposed to either antioxidant or inhibitor, no other vascular responses were performed to prevent interactive effects.

Detection of Endothelial ROS Production by Fluorescence Analysis

To evaluate intravascular ROS, a subsection of coronary arterioles were cannulated as described above. In the absence of light, dihydroethidium (DHE, 10^{-4} M) was intraluminally infused for 20 min. The arterioles were then flushed with PSS for 20 min to wash all dye from the vessel lumen and pipettes. DHE easily permeates cell membranes and, when oxidized by O_2^-, is converted to fluorescent ethidium bromide that intercalates into nuclear DNA [27, 28]. After the washout period, the vessel chamber was placed on an Olympus BX51WI upright microscope and was briefly (2 s) illuminated with a mercury lamp using appropriate excitation and emission filters for detection of ethidium bromide fluorescence (480–550 nm bandpass, 590 nm barrier) and hydroethidine fluorescence (330–385 nm bandpass, 590 nm barrier).

To quantify ROS-associated fluorescence in the arteriolar wall, a user-defined region of interest (ROI) box (10 × 100 μm) was placed vertically on the endothelial cell layer of the brightfield image. As shown in Table 1, the wall thickness of coronary arterioles from both groups were approximately 16 μm in width; therefore, the ROI box positively encompassed the entire endothelial cell layer and most of the smooth muscle layer. This excluded any adventitial tissue inclusion in mean fluorescence calculations. In theory, any differences among vessels in the extent of cellular hydroethidine loading could also lead to

Table 1 Animal and vessel characteristics for sham-control and nano-TiO_2 rats

	Sham-control	Nano-TiO_2
Animal characteristics		
Number of rats (*n*)	$n = 33$	$n = 50$
Age (weeks)	10.8 ± 2	11.1 ± 2
Body weight (g)	330 ± 6	359 ± 3*
Heart weight (mg)	1056 ± 17	1103 ± 13*
LV weight (mg)	798 ± 13	837 ± 10*
LV/HW ratio	0.758 ± 0.004	0.761 ± 0.006
Dry heart weight (mg)	207 ± 5	227 ± 1*
Dry LV weight (mg)	163 ± 3	176 ± 6*
Vessel characteristics		
Normal superfusate		
Number of vessels (*n*)	$n = 33$	$n = 46$
Maximal diameter (μm)	161 ± 3	156 ± 3
Wall thickness (μm)	17 ± 0.5	16 ± 0.4
Initial steady-state diameter (μm)	113 ± 5	108 ± 5
Spontaneous tone (%)	28 ± 3	30 ± 3
Superfusate with L-NMMA		
Number of vessels (*n*)	$n = 7$	$n = 6$
Initial steady-state diameter (μm)	79 ± 12	98 ± 12
Spontaneous tone (%)	50 ± 6†	36 ± 6*†
Superfusate with indomethacin		
Number of vessels (*n*)	$n = 10$	$n = 17$
Initial steady-state diameter (μm)	83 ± 8	83 ± 9
Spontaneous tone (%)	46 ± 5†	47 ± 1†
Superfusate with tempo + catalase		
Number of vessels (*n*)	$n = 9$	$n = 8$
Initial steady-state diameter (μm)	107 ± 7	102 ± 18
Spontaneous Tone (%)	38 ± 4	38 ± 9

Values are means ± S.E. * $P \leq 0.05$ sham-control versus nano-TiO_2, † $P \leq 0.05$ significant treatment effect within group

differences in ethidium bromide fluorescence that would be erroneously interpreted as differences in ROS. Therefore, subtracting the ethidium bromide image from the hydroethidine image represents the DHE that has been intercalated into the DNA. The ROI was then superimposed onto the subtracted fluorescent image in order to acquire mean fluorescence on the endothelial cell layer rather than the smooth muscle cell layer of each vessel. Total fluorescence intensity was calculated as average fluorescence intensity per pixel x surface area using Microsuite software analysis program (Olympus).

ACh-Induced Vasodilation

To determine the role of ROS, NO, and PG as a mechanism for impaired vasodilation to ACh in coronary arterioles after nano-TiO_2 exposure, vascular responses to ACh (1×10^{-9}–1×10^{-4} M) were examined in the presence or absence of 2,2,6,6-tetramethylpiperidine-N-oxyl (TEMPOL, 1×10^{-4} M) and catalase (50 units/mL), N^G-monomethyl-L-arginine (L-NMMA, 1×10^{-4} M), or indomethacin (1×10^{-5} M). We have previously shown that the TEMPOL concentration used in the current study diminishes DHE fluorescence [29].

Arachidonic Acid-Induced Vasoreactivity

To evaluate inflammatory-related vasoreactivity, vascular responses to arachidonic acid (1×10^{-10}–1×10^{-6} M) were evaluated in coronary arterioles from sham-control and rats exposed to nanoparticles. Metabolites of arachidonic acid, such as thromboxane, can influence the basal tone and reactivity of coronary arterioles. In another set of arterioles, vasoconstriction to U46619 (1×10^{-9} – 1×10^{-5} M), a thromboxane receptor ($T \times A_2$) analog, was evaluated from both groups. At the conclusion of each experiment, vessels were washed with Ca^{2+}-free PSS for thirty minutes to obtain maximal passive diameter and wall thickness at 45 mm Hg.

Heart Weight Measurements

After dissection of coronary arterioles, atrias were trimmed off and wet weights of right and left ventricles (heart weight) and left ventricles including the septum (left ventricle weight) were measured. The ventricles were then placed in a desiccator for a minimum of 3 days to acquire dry weights of the heart and left ventricle.

Formulas and Statistical Analysis

Data are expressed as means ± standard error. Spontaneous tone was calculated by the following equation:

$$\text{Spontaneous tone } (\%) = [(D_M - D_I)/D_M] \times 100$$

where D_M is the maximal diameter recorded at 45 mm Hg under Ca^{2+}-free PSS as described above, and D_I is the initial steady-state diameter achieved prior to experimental period. Vessels were used for experiments only if spontaneous tone ≥20% was achieved.

The experimental responses to ACh and arachidonic acid are expressed using the following equation:

$$\text{Relaxation } \% = [(D_{SS} - D_{Con})/(D_M - D_{Con})] \times 100$$

where D_{SS} is the steady-state arteriolar diameter during the experimental period, and D_{Con} is the control diameter recorded immediately prior to experimental period. All

experimental periods were at least 3 min in duration, and all steady-state diameters were collected for at least a one-minute period. Vasodilation is represented as "% relaxation" because this equation normalizes for potential differences in baseline diameter at the start of a response curve.

The experimental responses to U46619 are expressed using the following equation:

$$\text{Constriction } \% = [(D_{\text{Con}} - D_{\text{SS}})/(D_{\text{Con}})] \times 100$$

Concentration-diameter curves were evaluated by two-way repeated measures ANOVA in order to detect differences within and between factors. Pairwise comparisons were made by post hoc analysis (Bonferroni) when a significant main effect was found. T-tests were used for comparisons of animal and vessel characteristics and mean fluorescence. Significance was set at $P \leq 0.05$.

Results

Animal and Vessel Characteristics

Body weight, heart weight, and left ventricle weights (wet and dry) were increased in rats exposed to nano-TiO_2 compared to sham-control (Table 1). However, these latter two effects appear to be largely due to differences in body weight because the ratio of the left ventricle weights to total heart weights was not different among the two groups. Nano-TiO_2 exposure did not alter maximum diameter, wall thickness, or spontaneous arteriolar tone achieved prior to interventions compared to sham-control (Table 1). In coronary arterioles from sham-control rats, incubations with both L-NMMA and indomethacin increased spontaneous tone (Table 1). Whereas, in arterioles from rats exposed to

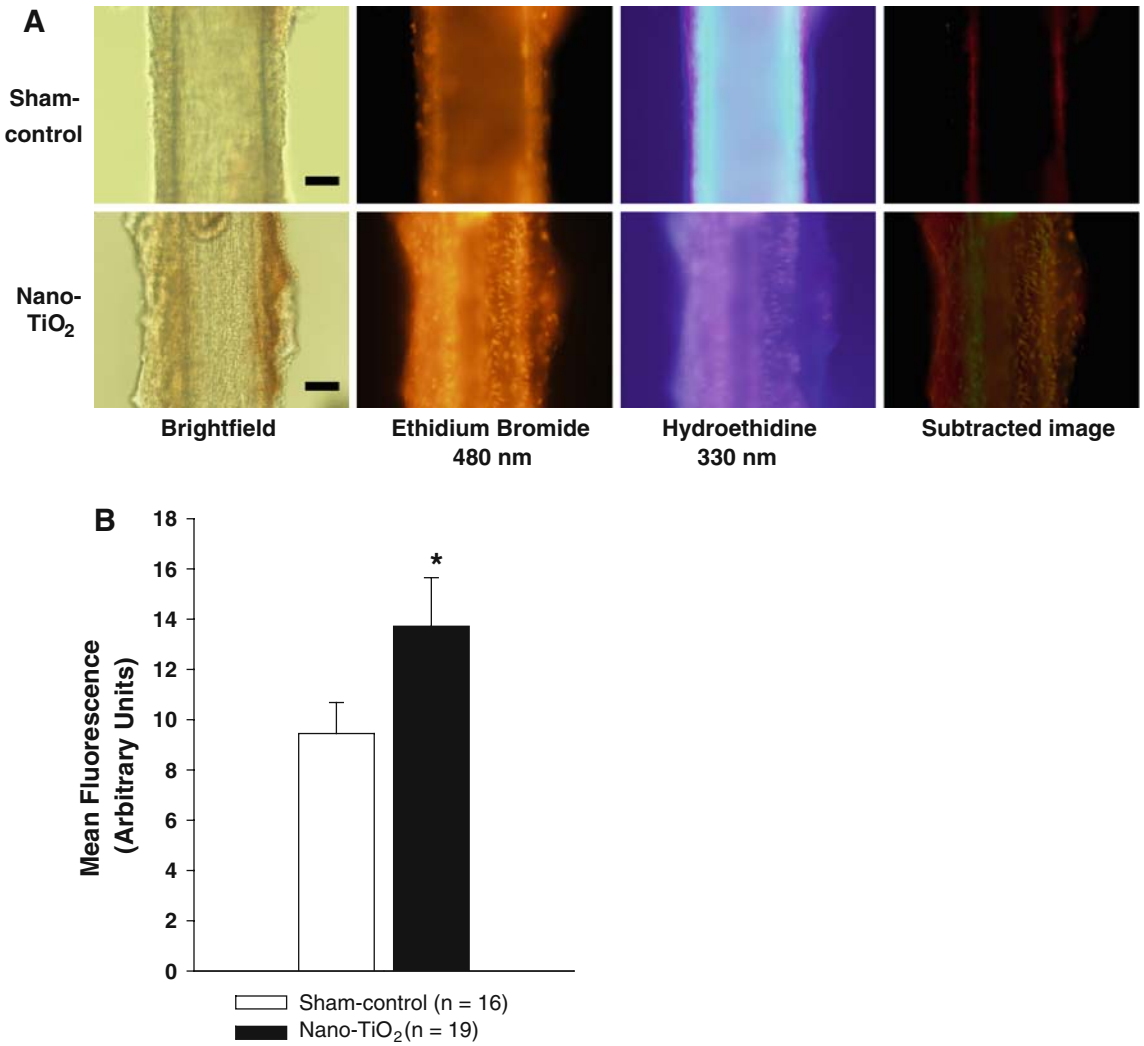

Fig. 1 **a** Representative images of coronary arterioles loaded with DHE from sham-control and nano-TiO_2 exposed rats. **b** Mean fluorescence calculated from ROI was significantly greater in coronary arterioles from rats exposed to nano-TiO_2 compared to sham-controls, indicating greater basal ROS generation. Values are means ± S.E. *, $P \leq 0.05$ sham-control versus nano-TiO_2

nano-TiO_2, spontaneous tone was increased after incubation with indomethacin only (Table 1).

Intravascular ROS Fluorescence

Representative brightfield and fluorescent photographs of coronary arterioles from sham-control, and nano-TiO_2 rats are presented in Fig. 1a. DHE treatment revealed a significant increase in ethidium bromide fluorescence (normalized to hydroethidine fluorescence) in the microvascular wall of arterioles from nano-TiO_2-exposed rats compared to sham-control rats (Fig. 1b). This increase in fluorescence is consistent with an elevation of ROS in the microvascular wall after nano-TiO_2 exposure.

Vasodilator Responses to ACh

Consistent with our previous report [2], ACh-induced vasodilation was impaired in coronary arterioles from rats exposed to nano-TiO_2 compared to sham-control rats (Fig. 2). Incubation with TEMPOL and catalase restored ACh-induced vasodilation in coronary arterioles from nano-TiO_2 rats (Fig. 2). This indicates that ROS inhibition can reverse the impairments in endothelium-dependent vasodilation in rats exposed to nano-TiO_2.

Contribution of NO and Prostaglandins to ACh-Induced Vasodilation

To determine the contribution of NO to ACh-induced vasodilation, vascular responses to ACh were performed before and during incubation with the NOS inhibitor L-NMMA. Incubation with indomethacin was performed in a separate set of arterioles to determine the contribution of prostaglandins (PG) to ACh-induced vasodilation. Following incubation with L-NMMA or indomethacin, ACh-induced vasodilation was abolished in arterioles from sham-control rats but neither altered vasodilation in coronary arterioles from nano-TiO_2 rats (Fig. 3). This indicates that in sham-control rats, coronary arterioles are dependent upon both NO and PG to mediate ACh-induced vasodilation. Additionally, these data indicate that coronary arterioles from rats exposed to nano-TiO_2 display dysfunctional NO and PG-dependent dilator mechanisms.

Vasodilation to Arachidonic Acid

The metabolism of arachidonic acid can produce both vasoconstrictors and vasodilators [19]. In order to determine the contribution of arachidonic acid metabolism on vascular tone and reactivity, vasoreactivity in response to arachidonic acid was evaluated in coronary arterioles from both sham-control and nano-TiO_2-exposed rats. Coronary arterioles from rats exposed to nano-TiO_2 exhibited a slight vasoconstrictor response to arachidonic acid (Fig. 4a), whereas arterioles from sham-control rats dilated. This suggests that nano-TiO_2 exposure may facilitate the overproduction of vasoconstrictor metabolites of arachidonic acid and/or impair the production of vasodilatory mediators.

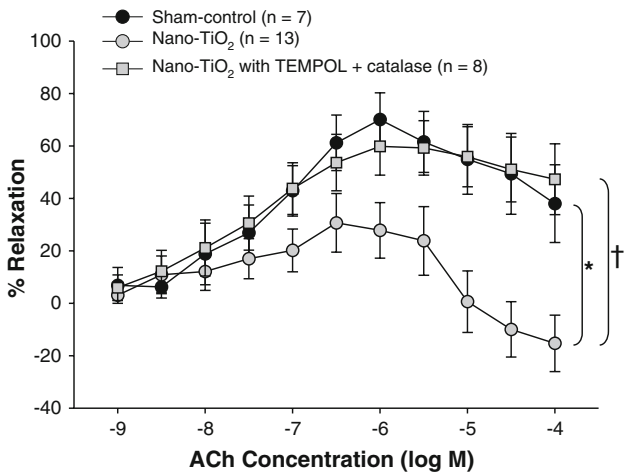

Fig. 2 ACh-induced vasodilation was impaired in coronary arterioles from rats exposed to nano-TiO_2 compared to sham-controls. After a 30-min preincubation with TEMPOL (1×10^{-4} M) and catalase (50 units/mL), vasodilation in response to ACh was restored in coronary arterioles from rats exposed to nano-TiO_2. Values are means ± S.E. * $P \leq 0.05$ sham-control vs. nano-TiO_2. † $P \leq 0.05$ significant treatment effect within group

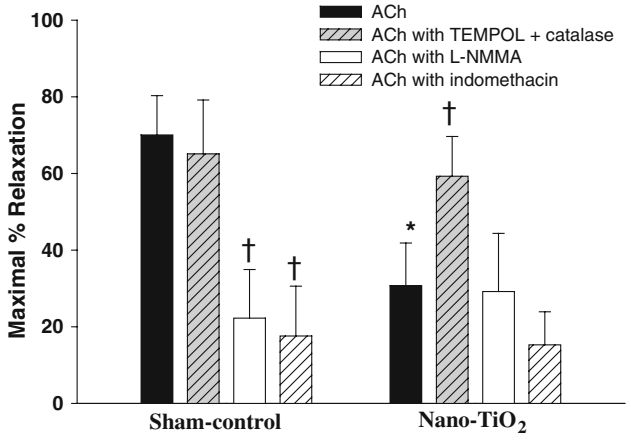

Fig. 3 Maximal dilation in response to ACh in the presence of normal superfusate, TEMPOL (1×10^{-4} M) and catalase (50 units/mL), L-NMMA (1×10^{-4} M), or indomethacin (1×10^{-5} M) in coronary arterioles from sham-control and nano-TiO_2 exposed rats. Incubation with L-NMMA or indomethacin decreased the ACh-induced vasodilation in arterioles from sham-control rats, but did not alter maximal dilation from nano-TiO_2 rats. Values are means ± S.E. * $P \leq 0.05$ sham-control vs. nano-TiO_2. † $P \leq 0.05$ significant treatment effect within group

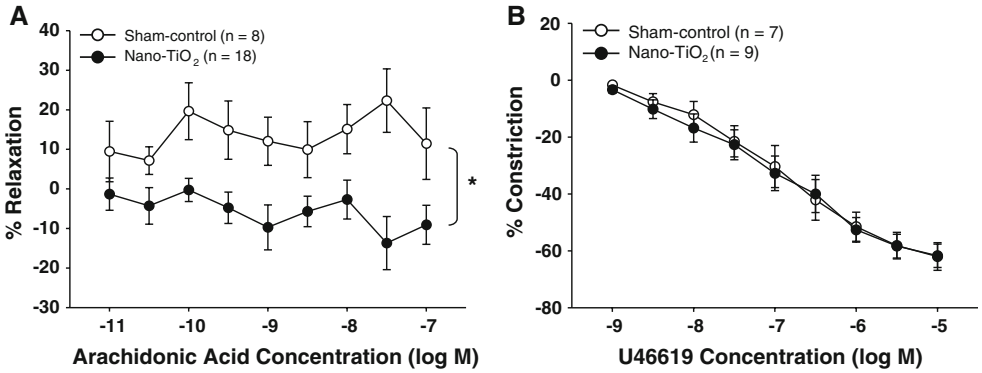

Fig. 4 **a** Nano-TiO_2 inhalation caused a slight, but significant vasoconstriction in coronary arterioles in response to arachidonic acid compared to vasodilation observed in sham-control rats. **b** There were no group differences in the vasoconstriction of coronary arterioles in response to the TxA_2 analog U46619. Values are means ± S.E. * $P \leq 0.05$ sham-control versus nano-TiO_2

Thromboxane-Induced Vasoconstriction

To determine the contribution of a vasoconstrictor metabolite of arachidonic acid to the vasoreactivity of coronary arterioles, constriction in response to U46619, a TxA_2 analog, was assessed in arterioles from sham-control and nano-TiO_2 rats. There were no differences in vasoconstrictor responses to U46619 in arterioles from either group (Fig. 4b). This indicates that the microvascular responsiveness to thromboxane is not altered after nano-TiO_2 inhalation.

Discussion

The major findings from this study are the following: (1) nano-TiO_2 exposure increases coronary arteriolar ROS, (2) nano-TiO_2 exposure impairs endothelium-dependent vasodilation, and this impairment is restored by incubation with ROS scavengers, (3) inhibition of NOS or COX inhibits arteriolar vasodilation in response to ACh in arterioles from sham-control rats, but not from nano-TiO_2-exposed rats, and (4) arachidonic acid causes slight vasoconstriction in coronary arterioles from rats exposed to nano-TiO_2, but dilation of microvessels from sham-control rats. These particle-dependent findings relate to human studies in that they have similarly shown an increase in free radical generation in coronary dysfunction during pathological states such as ischemia and MI [4–6]. Considered together, it is attractive to speculate that the net result would be an augmentation of cardiac dysfunction.

The first critical finding in the current study is that intravascular ROS, as visualized by DHE, is greater in coronary arterioles from rats exposed to nano-TiO_2 (Fig. 1). This is in agreement with previous reports from our laboratory which showed that inhalation of either fine or nano-TiO_2 caused an enhanced ROS fluorescence in arterioles from the spinotrapezius muscle [21]. As proposed by Okayama et al. [30], one possible mechanism for particle-induced cardiac functional changes is an altered role of ROS. Specifically, these investigators showed that exposure to diesel exhaust particles (DEP) led to increased O_2^- production in rat cardiac myocytes in a concentration and time-dependent manner. Several other studies have concluded that particle exposure can induce ROS generation, specifically O_2^- and H_2O_2, causing significant dysfunction in aortic rings in vitro [31–33]. Therefore, it is plausible that pharmacologically scavenging ROS with TEMPOL and catalase would ameliorate the impairment of endothelium-dependent arteriolar vasodilation associated with nanoparticle inhalation.

The second major finding from this study was that incubation of coronary arterioles with ROS scavengers, TEMPOL and catalase, restored endothelium-dependent dilation in rats exposed to nano-TiO_2 (Fig. 2). Our laboratory has previously shown that incubation with TEMPOL, a membrane soluble SOD mimetic which converts O_2^- to H_2O_2; and catalase, which converts H_2O_2 to water and oxygen, partially restores both arteriolar endothelium-dependent dilation and NO production in the rat spinotrapezius muscle microcirculation after nanoparticle inhalation [21]. It has been proposed that particle-induced oxidative stress is imposed by unfettered NO/NOS production and activity and subsequent conversion to O_2^- and eventually H_2O_2 [33, 34]. Indeed, Knuckles et al. [35] have suggested that an uncoupling of eNOS is the most likely mechanism for increased vasoconstriction after mesenteric arteries and veins were exposed to whole diesel exhaust. H_2O_2 can be generated as quickly as one minute after the treatment of human pulmonary artery endothelial cells with particles and can cause significant pulmonary artery vasoconstriction [32]. However, Miller et al. [36] recently showed that coincubation with SOD could completely reverse the inhibitory effect of 10 μg/mL DEP on ACh-induced vasodilation in aortic rings. Additionally, TEMPOL administration during inhalation exposure to gasoline-exhaust emissions attenuates increases in oxidative stress, as determined by the thiobarbituric acid reactive substances (TBARS) assay in the mouse aorta [37]. Likewise, SOD and catalase pretreatment can significantly decrease DEP-induced cell

damage in cardiac myocytes compared to DEP-treatment in the absence of these antioxidant enzymes [30]. Collectively, these studies indicate that particle exposure induces vascular dysfunction via ROS generation, and this can be diminished by incubation with ROS scavengers.

The third major finding from the present study was that ACh-induced vasodilation in coronary arterioles from sham-control rats was significantly impaired in the presence of NOS or COX inhibitors, but this effect was not present in rats exposed to nano-TiO_2. This indicates that nanoparticle exposure impairs both NO and PG-dependent vasodilator mechanisms (Fig. 3). This is consistent with previous studies from our laboratory and others which report that particle exposure impairs NO-dependent vasodilation in a variety of vascular locations, such as pulmonary [38], coronary [39], and skeletal muscle [8, 21]. Cherng et al. [39] proposed that the impaired vasodilator capacity in septal arteries after DE exposure was NO-dependent, which was suggested to normally oppose potent vasoconstriction by endothelin-1 in healthy vessels. However, the contribution of a COX-derived vasodilator was not evaluated. The impairment of endogenous NO after nanoparticle exposure is further corroborated in the present study owing to the heightened spontaneous tone in arterioles from sham-control after L-NMMA incubation compared to rats exposed to nano-TiO_2 (Table 1). This indicates that NO contributes significantly not only to the coronary microvascular reactivity, but also to the establishment of basal tone in these vessels. Moreover, these contributions are compromised after nanoparticle inhalation. Because indomethacin treatment increased spontaneous arteriolar tone in both groups (Table 1), but decreased ACh-induced dilation only in arterioles from sham-control rats (Fig. 3); it is important to reiterate that the mechanisms that govern basal tone do not implicitly alter arteriolar vasoactive function in response to a given stimuli.

The present results also indicate that compared to the dilation observed in sham-control microvessels, nano-TiO_2 exposure caused a slight vasoconstriction in coronary arterioles in response to arachidonic acid (Fig. 4a). Therefore, we suggest that inhalation of nano-sized particles also induces a loss of arachidonic acid metabolite vasodilators. More precisely, it appears as though nanoparticle inhalation instigates a conversion to arachidonic acid-dependent vasoconstriction, while also initiating ROS generation in coronary arterioles. To better characterize the former possibility, the arachidonic acid metabolite thromboxane was evaluated in the present study. Although previous research shows that chronic exposure to the particulate phase of smoke induced elevates platelet thromboxane formation [40], the present study found that nanoparticle exposure does not alter arteriolar vasoconstriction in response to the TxA_2 analog U46619 (Fig. 4b). Because TxA_2 production was not evaluated, we cannot currently conclude that TxA_2 activity is not altered by nanoparticle exposure. Ideally, a long-term inhalation study would be necessary to perturb the thromboxane pathway and subsequent vasoactive response. However, other possible sources of arachidonic acid-mediated vasoconstriction could contribute to nanoparticle-induced alterations in vasoreactivity. For example, the cytochrome p-450 pathway, specifically 20-HETE, and also certain prostaglandins (PGF_{2alpha}, PGH_2) can function as vasoconstrictors and are common products of arachidonic acid metabolism [19]. Increases in coronary vascular resistance and subsequent reduction in myocardial perfusion have been shown to contribute to myocardial ischemia after particle inhalation [14]. Therefore, the contributions of these arachidonic acid-mediated vasoconstrictors to coronary arteriolar function after nanoparticle exposure must be defined by further investigation.

As previously reported, we estimate that in the occupational setting, it would take a typical worker 5 years to achieve a similar pulmonary burden equivalent to the 10 μg burdens used herein [2, 21]. This alone may in first consideration appear unrealistic. However, given that: aerosol concentrations encountered in the workplace can easily exceed those used in the current study (6 mg/m^3); our calculation of 5 years was based upon sedentary pulmonary function; the bioretention of inhaled particles is quite variable; not all workers are young and/or healthy; and typical occupational careers exceed 5 years, the burdens used in this study may have not only occupational relevance, but also personal or environmental relevance.

We first characterized the particle-dependent impairments of endothelium-dependent arteriolar dilation in the systemic microcirculation in 2004 [41]. These observations were also coupled to a large increase in rolling and adhering polymorphonuclear leukocytes in the venular circuit [42]. While these initial observations were made with exposures to larger, fine TiO_2, and residual oil fly ash, we later showed that exposure to nano-TiO_2 at similar mass depositions produced a far more robust impairment of microvascular reactivity [8]. In all of these studies, pulmonary status was evaluated by bronchoalveolar lavage and histology. At lung burdens used in the present study, the common pulmonary response was focalized alveolitis with no change in lavage markers of gross inflammation or damage. Taken together, this suggests that subsequent systemic effects are not due to the inherent toxicity of a given particle or pulmonary overload. Most recently, we have identified mechanisms in the arteriolar wall that compromise microvascular reactivity after nanoparticle exposure. Specifically, endogenous NO bioavailability is compromised, and this occurs in the presence of elevated

ROS and reactive nitrogen species associated with NADPH oxidase activity and/or myeloperoxidase activity [21]. The logical extension of these serial studies is to determine whether a similar toxicity results in critical organs such as the heart (in effort to more directly link particle exposure with cardiovascular morbidity and mortality). This was first shown with subepicardial arterioles from rats exposed to nano-TiO_2 [2]. In these studies, we were able to make such a link and verify that a similar level microvascular dysfunction occurs in the heart after pulmonary nanoparticle exposure. The current study strengthens our initial findings in the coronary microcirculation and offers potential mechanisms by which this effect manifests itself.

Conclusions

Mechanistic studies evaluating the adverse cardiovascular effects of nanoparticles remain limited. We and others have focused on the functional and structural changes that occur in the systemic and pulmonary vasculature, and we collectively report that alterations in vasoreactivity occur in humans [43] and animals alike [8, 21, 42, 44] following particle exposure. The current study defines a mechanistic link between nanoparticle inhalation and subsequent endothelium-dependent dysfunction in the coronary microcirculation. Specifically, an increase in microvascular wall ROS appears to contribute to the impairment of ACh-induced vasodilation in rats exposed to nano-TiO_2, since this dysfunction can be attenuated by local ROS scavenging. Such adverse cardiac functional changes (induced by particle exposure) have been linked to altered cellular mechanisms associated with NOS uncoupling and subsequent ROS generation. The present findings mark a critical step in identifying the negative effects of nanoparticle exposure in the heart. Additional nanoparticles such as carbon nanotubes must be characterized in future studies as nano-TiO_2 has been herein. This is necessary because no single nanoparticle is ideally representative of the greater lot of tremendously diverse nanoparticles. Similarly, additional tissues must be evaluated because toxicity in one tissue does not implicitly define identical toxicity (if any) in another tissue.

Acknowledgments The authors thank Carroll McBride and Kimberly Wix for their expert technical assistance in this study, and Travis Knuckles, Ph.D., for his help in reviewing this manuscript. This work was supported by the National Institutes of Health/National Institute for Environmental Health Sciences [grant numbers R01-ES015022 and RC1 ES018274 (to TRN)].

Disclaimer The findings and conclusions in this report are those of the authors and do not necessarily represent the views of the National Institute for Occupational Safety and Health.

References

1. LaDou, J. (2004). The asbestos cancer epidemic. *Environmental Health Perspectives, 112*, 285–290.
2. LeBlanc, A. J., Chen, B. T., Frazer, D., Castronova, V., & Nurkiewicz, T. R. (2009). Nanoparticle inhalation impairs endothelium-dependent vasodilation in subepicardial arterioles. *Journal of Toxicology and Environmental Health Part A, 72*, 1576–1584.
3. Araujo, J. A., Barajas, B., Kleinman, M., Wang, X., Bennett, B. J., Gong, K. W., et al. (2008). Ambient particulate pollutants in the ultrafine range promote early atherosclerosis and systemic oxidative stress. *Circulation Research, 102*, 589–596.
4. Garlick, P. B., Davies, M. J., Hearse, D. J., & Slater, T. F. (1987). Direct detection of free radicals in the reperfused rat heart using electron spin resonance spectroscopy. *Circulation Research, 61*, 757–760.
5. Ferrari, R., Ceconi, C., Curello, S., Guarnieri, C., Caldarera, C. M., Albertini, A., et al. (1985). Oxygen-mediated myocardial damage during ischaemia and reperfusion: Role of the cellular defences against oxygen toxicity. *Journal of Molecular and Cellular Cardiology, 17*, 937–945.
6. Grech, E. D., Dodd, N. J., Jackson, M. J., Morrison, W. L., Faragher, E. B., & Ramsdale, D. R. (1996). Evidence for free radical generation after primary percutaneous transluminal coronary angioplasty recanalization in acute myocardial infarction. *American Journal of Cardiology, 77*, 122–127.
7. Dreher, K. L. (2004). Health and environmental impact of nanotechnology: Toxicological assessment of manufactured nanoparticles. *Toxicological Sciences, 77*, 3–5.
8. Nurkiewicz, T. R., Porter, D. W., Hubbs, A. F., Cumpston, J. L., Chen, B. T., Frazer, D. G., et al. (2008). Nanoparticle inhalation augments particle-dependent systemic microvascular dysfunction. *Particle and Fibre Toxicology, 5*, 1.
9. Oberdorster, G. (1996). Significance of particle parameters in the evaluation of exposure-dose–response relationships of inhaled particles. *Inhalation Toxicology, 8*(Suppl), 73–89.
10. Weisfeldt, M. L., Wright, J. R., Shreiner, D. P., Lakatta, E., & Shock, N. W. (1971). Coronary flow and oxygen extraction in the perfused heart of senescent male rats. *Journal of Applied Physiology, 30*, 44–49.
11. Qi, X. L., Nguyen, T. L., Andries, L., Sys, S. U., & Rouleau, J. L. (1998). Vascular endothelial dysfunction contributes to myocardial depression in ischemia–reperfusion in the rat. *Canadian Journal of Physiology and Pharmacology, 76*, 35–45.
12. Cozzi, E., Hazarika, S., Stallings, H. W., III, Cascio, W. E., Devlin, R. B., Lust, R. M., et al. (2006). Ultrafine particulate matter exposure augments ischemia–reperfusion injury in mice. *American Journal of Physiology. Heart and Circulatory Physiology, 291*, H894–H903.
13. Libby, P., & Theroux, P. (2005). Pathophysiology of coronary artery disease. *Circulation, 111*, 3481–3488.
14. Bartoli, C. R., Wellenius, G. A., Coull, B. A., Akiyama, I., Diaz, E. A., Lawrence, J., et al. (2009). Concentrated ambient particles alter myocardial blood flow during acute ischemia in conscious canines. *Environmental Health Perspectives, 117*, 333–337.
15. Kim, C., Kim, J. Y., & Kim, J. H. (2008). Cytosolic phospholipase A(2), lipoxygenase metabolites, and reactive oxygen species. *BMB Reports, 41*, 555–559.
16. Wang, P., Chen, H., Qin, H., Sankarapandi, S., Becher, M. W., Wong, P. C., et al. (1998). Overexpression of human copper, zinc-superoxide dismutase (SOD1) prevents postischemic injury. *Proceedings of the National Academy of Sciences of the United States of America, 95*, 4556–4560.

17. Bondy, S. C., & Naderi, S. (1994). Contribution of hepatic cytochrome P450 systems to the generation of reactive oxygen species. *Biochemical Pharmacology, 48*, 155–159.
18. Rosenblum, W. I. (1987). Hydroxyl radical mediates the endothelium-dependent relaxation produced by bradykinin in mouse cerebral arterioles. *Circulation Research, 61*, 601–603.
19. Roman, R. J. (2002). P-450 metabolites of arachidonic acid in the control of cardiovascular function. *Physiological Reviews, 82*, 131–185.
20. Saitoh, S., Zhang, C., Tune, J. D., Potter, B., Kiyooka, T., Rogers, P. A., et al. (2006). Hydrogen peroxide: a feed-forward dilator that couples myocardial metabolism to coronary blood flow. *Arteriosclerosis, Thrombosis, and Vascular Biology, 26*, 2614–2621.
21. Nurkiewicz, T. R., Porter, D. W., Hubbs, A. F., Stone, S., Chen, B. T., Frazer, D. G., et al. (2009). Pulmonary nanoparticle exposure disrupts systemic microvascular nitric oxide signaling. *Toxicological Sciences, 110*, 191–203.
22. Hurum, D. C., Gray, K. A., Rajh, T., & Thurnauer, M. C. (2005). Recombination pathways in the Degussa P25 formulation of TiO2: surface versus lattice mechanisms. *The Journal of Physical Chemistry. B, 109*, 977–980.
23. Vasiliev, P. O., Faure, B., Ng, J. B., & Bergstrom, L. (2008). Colloidal aspects relating to direct incorporation of TiO2 nanoparticles into mesoporous spheres by an aerosol-assisted process. *Journal of Colloid and Interface Science, 319*, 144–151.
24. Brunauer, S., Emmett, P. H., & Teller, E. (1938). Adsorption of gases in multimolecular layers. *Journal of the American Chemical Society, 60*, 309–319.
25. Sager, T. M., Kommineni, C., & Castranova, V. (2008). Pulmonary response to intratracheal instillation of ultrafine versus fine titanium dioxide: role of particle surface area. *Particle and Fibre Toxicology, 5*, 17.
26. Chilian, W. M., Eastham, C. L., & Marcus, M. L. (1986). Microvascular distribution of coronary vascular resistance in beating left ventricle. *American Journal of Physiology, 251*, H779–H788.
27. Benov, L., Sztejnberg, L., & Fridovich, I. (1998). Critical evaluation of the use of hydroethidine as a measure of superoxide anion radical. *Free Radical Biology and Medicine, 25*, 826–831.
28. Morgan, A. R., Evans, D. H., Lee, J. S., & Pulleyblank, D. E. (1979). Review: Ethidium fluorescence assay Part II. Enzymatic studies and DNA–protein interactions. *Nucleic Acids Research, 7*, 571–594.
29. Nurkiewicz, T. R., & Boegehold, M. A. (2007). High salt intake reduces endothelium-dependent dilation of mouse arterioles via superoxide anion generated from nitric oxide synthase. *American Journal of Physiology: Regulatory, Integrative and Comparative Physiology, 292*, R1550–R1556.
30. Okayama, Y., Kuwahara, M., Suzuki, A. K., & Tsubone, H. (2006). Role of reactive oxygen species on diesel exhaust particle-induced cytotoxicity in rat cardiac myocytes. *J Toxicol Environ Health A, 69*, 1699–1710.
31. Wang, T., Chiang, E.T., Moreno-Vinasco, L., Lang, G.D., Pendyala, S., Samet, J.M., et al. (2009). Particulate matter disrupts human lung endothelial barrier integrity via ROS- and p38 MAPK-dependent pathways. *American Journal of Respiratory Cell and Molecular Biology*. [Epub ahead of print] PMID: 19520919.
32. Li, Z., Hyseni, X., Carter, J. D., Soukup, J. M., Dailey, L. A., & Huang, Y. C. (2006). Pollutant particles enhanced H2O2 production from NAD(P)H oxidase and mitochondria in human pulmonary artery endothelial cells. *American Journal of Physiology. Cell Physiology, 291*, C357–C365.
33. Ying, Z., Kampfrath, T., Thurston, G., Farrar, B., Lippmann, M., Wang, A., et al. (2009). Ambient particulates alter vascular function through induction of reactive oxygen and nitrogen species. *Toxicological Sciences, 111*, 80–88.
34. Bai, Y., Suzuki, A. K., & Sagai, M. (2001). The cytotoxic effects of diesel exhaust particles on human pulmonary artery endothelial cells in vitro: Role of active oxygen species. *Free Radical Biology and Medicine, 30*, 555–562.
35. Knuckles, T. L., Lund, A. K., Lucas, S. N., & Campen, M. J. (2008). Diesel exhaust exposure enhances venoconstriction via uncoupling of eNOS. *Toxicology and Applied Pharmacology, 230*, 346–351.
36. Miller, M. R., Borthwick, S. J., Shaw, C. A., McLean, S. G., McClure, D., Mills, N. L., et al. (2009). Direct impairment of vascular function by diesel exhaust particulate through reduced bioavailability of endothelium-derived nitric oxide induced by superoxide free radicals. *Environmental Health Perspectives, 117*, 611–616.
37. Lund, A. K., Lucero, J., Lucas, S., Madden, M. C., McDonald, J. D., Seagrave, J. C., et al. (2009). Vehicular emissions induce vascular MMP-9 expression and activity associated with endothelin-1-mediated pathways. *Arteriosclerosis, Thrombosis, and Vascular Biology, 29*, 511–517.
38. Courtois, A., Andujar, P., Ladeiro, Y., Baudrimont, I., Delannoy, E., Leblais, V., et al. (2008). Impairment of NO-dependent relaxation in intralobar pulmonary arteries: Comparison of urban particulate matter and manufactured nanoparticles. *Environmental Health Perspectives, 116*, 1294–1299.
39. Cherng, T. W., Campen, M. J., Knuckles, T. L., Gonzalez Bosc, L., & Kanagy, N. L. (2009). Impairment of coronary endothelial cell ET(B) receptor function after short-term inhalation exposure to whole diesel emissions. *American Journal of Physiology: Regulatory, Integrative and Comparative Physiology, 297*(3):R640–R647.
40. Sherratt, A. J., Culpepper, B. T., & Lubawy, W. C. (1988). Relative participation of the gas phase and total particulate matter in the imbalance in prostacyclin and thromboxane formation seen following chronic cigarette smoke exposure. *Prostaglandins Leukotrienes and Essential Fatty Acids, 34*, 15–18.
41. Nurkiewicz, T. R., Porter, D. W., Barger, M., Castranova, V., & Boegehold, M. A. (2004). Particulate matter exposure impairs systemic microvascular endothelium-dependent dilation. *Environmental Health Perspectives, 112*, 1299–1306.
42. Nurkiewicz, T. R., Porter, D. W., Barger, M., Millecchia, L., Rao, K. M., Marvar, P. J., et al. (2006). Systemic microvascular dysfunction and inflammation after pulmonary particulate matter exposure. *Environmental Health Perspectives, 114*, 412–419.
43. Brook, R. D., Brook, J. R., Urch, B., Vincent, R., Rajagopalan, S., & Silverman, F. (2002). Inhalation of fine particulate air pollution and ozone causes acute arterial vasoconstriction in healthy adults. *Circulation, 105*, 1534–1536.
44. Batalha, J. R., Saldiva, P. H., Clarke, R. W., Coull, B. A., Stearns, R. C., Lawrence, J., et al. (2002). Concentrated ambient air particles induce vasoconstriction of small pulmonary arteries in rats. *Environmental Health Perspectives, 110*, 1191–1197.